Layered Coordination Architecture for Resilient Restoration of Power Distribution Systems

Rabayet Sadnan, *Student Member, IEEE*, Shiva Poudel, *Member, IEEE*, Anamika Dubey, *Senior Member, IEEE*, and Kevin P. Schneider, *Fellow, IEEE*

Abstract— The current practices for restoring critical services in the distribution system during a disaster align with the traditional centralized ideology of distribution systems operations. A central processor evaluates the distribution system after a disruption and attains a restoration plan. However, the centralized operational paradigm is susceptible to single-point failures, requires full situational awareness of the distribution system, and poses scalability challenges for large multi-feeder distribution systems. This motivates a distributed decision-making paradigm where multiple agents solve smaller sub-problems and jointly coordinate their individual decisions to achieve the global/network-level objective. Towards this goal, we propose a Layered Architecture for Distributed Algorithms for Resilience (LADAR) and a two-stage distributed algorithm for distribution system restoration. The proposed distributed decision-making framework enables the bottom-up restoration of the distribution system using all available resources, including distributed generation (DGs), while only requiring local awareness and limited communications with neighboring connected regions. The proposed framework is robust to single-point failures, enables autonomy using distributed algorithms, and had reduced computational cost compared to centralized optimization solutions.

Index Terms— Distributed optimization, layered architecture, power system restoration, resilience

NOMENCLATURE

A. Acronyms

DG	Distributed Generators
LADAR	Layered Architecture for Distributed Algorithms for Resilience
LC	Local Control
MILP	Mixed-Integer Linear Programming
SLEM	Switch-Level Equivalent Model
UA/DA	Upstream Area / Downstream Area

B. Sets

$\mathcal{E}$	Set of edges in a graph, $\mathcal{G}$
$\mathcal{E}_t$	Set of switches in a reduced-order graph, $\mathcal{G}_t$
$\mathcal{E}_{Fo}$	Set of faulted and open switches
$\mathcal{E}_c$	Set of switches in a cycle
$\mathcal{E}_{fed}$	Set of feeders
$\mathcal{E}_R$	Set of regulators
$\mathcal{E}_S$	Set of switchable lines
$\mathcal{E}_{Fc}$	Set of fault switches with closed state
$\mathcal{V}_S$	Set of switchable buses

$\mathcal{V}_t$	Set of buses in a reduced-order graph, $\mathcal{G}_t$
$\mathcal{V}_{area}$	Set of buses in an area
$\mathcal{E}_{area}$	Set of edges in an area
$\Phi=\{a, b, c\}$	Set of phases of a bus

C. Variables

δ_e	Switch decision variable
u_i	Load section energization variable
s_i	Load pick up variable
v_i	Node/Bus energization variable
w_i	Load priority
$\boldsymbol{P}_e + \mathrm{j}\boldsymbol{Q}_e$	Three-phase complex power flow in edge e
$\boldsymbol{P}_{Lj} + \mathrm{j}\boldsymbol{Q}_{Lj}$	Aggregated load for all phases at bus j
$\boldsymbol{U}_i$	Three-phase voltage magnitude square vector
$\boldsymbol{V}_i$	Three-phase voltage vector
U_i^ϕ	Voltage magnitude square at phase $\phi \in \Phi$
V_i^ϕ	Bus voltage at phase $\phi \in \Phi$
$q_{cap,i}^\phi$	Capacitance for phase $\phi \in \Phi$

D. Parameters

$\mathcal{P}_{Li}^\phi + \mathrm{j}\mathcal{Q}_{Li}^\phi$	Complex power demand for phase $\phi \in \Phi$ for bus i
$q_{cap,i}^{rated,\phi}$	Capacitor rating for phase $\phi \in \Phi$ at bus i
$\boldsymbol{S}_e^{rated}$	Apparent power flow limit for $e \in \mathcal{E}$
$\boldsymbol{S}_e$	Polygon based linearized equivalent of $\boldsymbol{S}_e^{rated}$
$\boldsymbol{P}_e^{max}$	Feeder/DGs power limit for Stage-I
$P_{2,B}/Q_{2,B}$	Power flow from the approximated slack node for Area B
$\mathbf{r}_e/\mathbf{x}_e$	Resistance/Reactance matrix of a line e
$\boldsymbol{U}^{min}/\boldsymbol{U}^{max}$	Minimum/maximum voltage magnitude square

I. INTRODUCTION

An increasing number of natural disasters and their impact on power distribution systems call for expedited incorporation of resilience [1]. Recent advances in the distribution systems, including the integration of DGs, microgrids, and distribution automation technologies, provide potential means to improve the resilience of distribution systems [2]–[4]. Traditionally, a centralized decision-support located at Advanced Distributed Management System (ADMS) is employed for restoration to coordinate line switches and other ADMS controllable DGs [4]. However, a central-only computing and decision-making paradigm poses several limitations due to the (i) requirement of full observability of the system to solve the optimal distribution system restoration (DSR) problem, (ii) vulnerability to single-point failure, and (iii) limited scalability to large systems with numerous controllable agents such as DGs, voltage regulators, etc. in central optimization approaches.

This has led to growing interest in distributed decision-making paradigms for power distribution systems operations

[5]. In such architectures, the decision-making process to restore the network is distributed among multiple agents such as microgrids, DGs, and intelligent switches. In related literature, this problem has been investigated from two different perspectives. First, distributed optimization algorithms have been proposed for network-level optimization using limited regional/local information and communications with neighboring nodes. Second, multi-agent systems (MAS) architectures have been proposed for information sharing, and coordination among distributed agents to coordinate decision-making [6]. The related literature on distributed optimization lacks in adequately defining the information-sharing structure among the distributed agents and tackling communication and computation-related challenges specific to the power distribution systems. Likewise, the existing literature on using MAS lacks practically viable and optimal algorithms for network-level distributed decision-making using local/regional information and limited neighbor communications [7], [8]. Additionally, power systems are safety-critical systems that require a certain level of visibility at the central location to implement/approve any decisions calling for coordination among centralized and distributed agents that are not explored in the context of resilience to extreme weather events. Additionally, there has been an extensive industry-led effort on developing and using standards for distribution-level monitoring and decision-making, including Common Information Model, MultiSpeak, and Open Field Message Bus (OpenFMB) to enable interoperability, portability, and scalability with growing penetrations of active nodes at the distribution-level [9]–[11]. These activities speak to the need for advanced architectures and algorithms to manage distribution-connected assets (for example, switches and DGs in restoration problems) in a real-world industrial environment. Within this context, we propose a layered coordination architecture for the resilient restoration of power distribution systems to address the aforementioned literature gaps. Furthermore, the adoption of the proposed laminar coordination architecture in developing restoration algorithms can help bridge the gap between theory and application practice of information sharing and decision-making in industrial environments, specifically power distribution systems. The proposed approach details an information-sharing framework appropriate for the safety-critical operations in power systems and a distributed optimization algorithm cognizant of communication-related constraints and time-sensitive decision-making requirements at the power distribution level.

A. Related Literature

Earlier methods for DSR focused on designing expert systems using heuristic search methods, and soft-computing algorithms [12], [13]. The use of feeder reconfiguration algorithms to restore the distribution system for local outages has been well-studied in the literature. Here, the restoration problem is modeled as a combinatorial optimization problem with operational and topological constraints [14]. Some of the recent work also included intentional islanding using microgrids and DGs to support the system's critical loads during extreme weather events [15]. Most of the existing literature assumes that a central controller is available at the distribution level

to collect data from all components and send out the control signals in a centralized fashion. Unfortunately, the existing approaches are computationally expensive, require a robust central controller to process the vast amount of data with high-speed communication capabilities, and poses scalability challenges for large multi-feeder distribution systems [16]. The limitations posed by the centralized methods have motivated the use of decentralized methods for restoration using multi-agent systems (MAS) [7], [17]. Advantages of MAS include the ability to survive single-point failures and decentralized data processing, which leads to efficient task distribution, resulting in faster operation and decision-making processes. However, the existing literature on using MAS is limited in connecting the actual decision-making protocols to the network-level optimal restoration problem and mechanism to converge to the optimal solutions in a distributed manner.

To this end, distributed optimization methods are promising solutions to solve network-level optimization problems by coordinating the optimal decisions of distributed agents. In a typical distributed operational environment, the central optimization problem is divided into several sub-problems to be independently solved by the distributed agents. Upon solving the local sub-problems, the distributed agents exchange information with neighboring agents, and the system reaches convergence over multiple communication rounds (macro-iterations). Recently, a generalized distributed optimization method - Alternating Direction Method of Multipliers (ADMM) has been widely used for power system applications such as load restoration, optimal power flow (OPF), and voltage control [6], [18]. However, the primary limitation of the ADMM-based methods is the high number of communication rounds (macro-iterations) needed for distributed agents to reach a consensus [6], [19]. Specifically for the restoration, a time-sensitive application, a high number of macro-iterations can lead to severe delays in the decision-making.

B. Proposed work and Contributions

This paper proposes a layered architecture, termed Layered Architecture for Distributed Algorithms for Resilience (LADAR), for the fast and scalable restoration of the power distribution systems and details the associated information exchange and decision-making processes.

The main contributions of the work are listed below.

- A layered architecture for distribution grid operations is proposed to enhance the resilience and support critical services, subject to faults(s) in the network. The proposed approach enables dynamically forming and self-organizing, resilient microgrids for distribution systems to supply power to the critical loads. An information-sharing framework is detailed for the network and measurement data at different layers of control hierarchy of the layered architecture using switch-level aggregated models and coordinated switch-level distributed and central decision-making.
- A hybrid approach is developed for DSR, based on the power distribution system's safety-critical requirements. The first stage, executed by ADMS, solves a max-flow problem for a reduced network to identify the optimal restored network topology by controlling the feeder-level switches. The

This article has been accepted for publication in a future issue of this journal, but has not been fully edited. Content may change prior to final publication. Citation information: DOI 10.1109/TII.2022.3177464, IEEE Transactions on Industrial Informatics

RABAYET *et al.*: LAYERED COORDINATION ARCHITECTURE FOR RESILIENT RESTORATION OF POWER DISTRIBUTION SYSTEMS   3

second stage, executed by local agents, solves a distributed optimal power flow problem to restore the network using local computations and communications with neighbors.

- A scalable distributed optimization method is developed for the restoration based on an equivalent area principle that requires a significantly small number of macro-iterations. The proposed LADAR approach are compared against traditional centralized optimization methods.

II. ARCHITECTURE & RESTORATION APPLICATION

The use of a layered decomposition approach for distributed optimization and control of physical infrastructure systems is elaborated in [9]. The layered framework can arguably provide (i) Extensibility–can be made to fit an existing grid structure, (ii) Boundary deference, (iii) Structural scalability, and (iv) Securability [9]. We propose a layered architecture for decision-support that synergistically combines centralized, distributed, and edge-control paradigms for resilient distributed restoration (see Fig. 1). Next, we develop a two-stage algorithm for restoration carried out by the agents located at different layers of the proposed architecture for decision-support. The proposed framework aligns with OpenFMB – state-of-the-art federated information sharing structure [20].

A. Three-Layer Architecture Framework for Decision-Support

The proposed layered architecture includes a centralized ADMS, many distributed decision-making agents, and local controllers to coordinate controllable devices, viz. tie and sectionalizing switches, DGs, and loads (see Fig. 1). Specifically, the LADAR framework has three layers of agents that can compute and coordinate the grid's controllable assets to support critical services and achieve network-level objectives.

1) Central ADMS (Layer-1): The Layer-1 agent, located at the ADMS, controls system-level devices such as tie and sectionalizing switches to obtain the restored network topology. The Layer-1 agent has limited access to network and measurement data with visibility to a switch-level aggregated distribution system model and measurements (total load and controllable DGs capacities). The switch-level aggregation leads to a reduced system represented for each switch-delimited areas, referred to as a switch-level equivalent model (SLEM) (Fig. 2b). Our rationale for using SLEM instead of the full network model at the Layer-1 agent is to alleviate the requirement for an expensive communication and data processing infrastructure needed for operational decision-making in a large distribution system with multiple feeders [10]. Instead, local federated information can be shared among distributed agents (Layer-2) to complement the central agent's decisions while simultaneously improving resilience to single-point failure [20]. However, central ADMS has the supervisory capabilities and authority to override the decisions of the distributed agents.

2) Distributed Agents (Layer-2): The Layer-2 agents are located at several distributed agents throughout the feeder. For the proposed LADAR architecture, the distributed agents
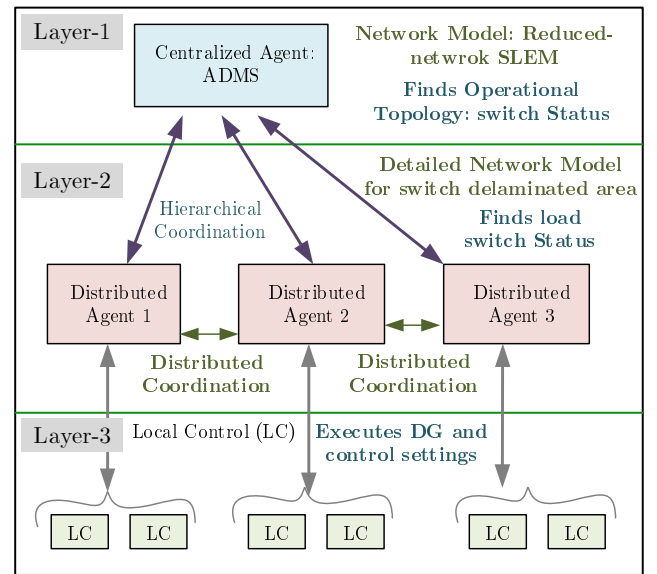

Fig. 1: Proposed LADAR Architecture

are located within the sectionalizer switch-delimited areas that can communicate with Layer-1 (hierarchical coordination) and neighboring Layer-2 agents (peer-to-peer communication). Layer-2 agents have access to the detailed feeder model for the local switch-delimited areas. These distributed agents use this information, communicate with neighboring Layer-2 agents, and attain optimal control actions for load and DG switches for restoration within their respective areas. The optimal actions are then carried out by the Layer-3 controllers.

3) Local Control (Layer-3): Layer-3 agents are device-level controllers located at each controllable node and communicate only with their respective Layer-2 agents in respective switch-delimited areas. These agents simply activate the required control modes in response to the control signals received from the respective Layer-2 agents for example optimal load switch statuses and DG set-points.

B. Restoration Application using LADAR Architecture

We propose a two-stage algorithm for restoration that aligns with the visibility and controllability of different levels of the proposed LADAR architecture (in Section II.A), and optimally employs the flexibility and resilience of the layered framework for operational decision-making.

1) Stages of Distributed Restoration: We propose a two-stage algorithm that aligns with the aforementioned layered coordination framework for the distribution system restoration with the ability to form intentional islands. Layer-1 agents carry out Stage-I, and Stage-II of the algorithm is implemented by the Layer-2 distributed agents. Here, 'Layers' refers to different control hierarchies (Fig.1), and 'Stage' refers to different phases of the proposed restoration algorithm. Stage-I solves for the optimal restored network tree/forest using SLEM by solving a centralized mixed-integer linear programming (MILP) problem. Stage-II optimizes for the granular control for loads and DGs for power balance and voltage constraint satisfaction using detailed network model and measurement data for the local areas. At both stages, the optimization problem is formulated as a MILP. However, instead of solving a large-scale computationally challenging MILP, smaller
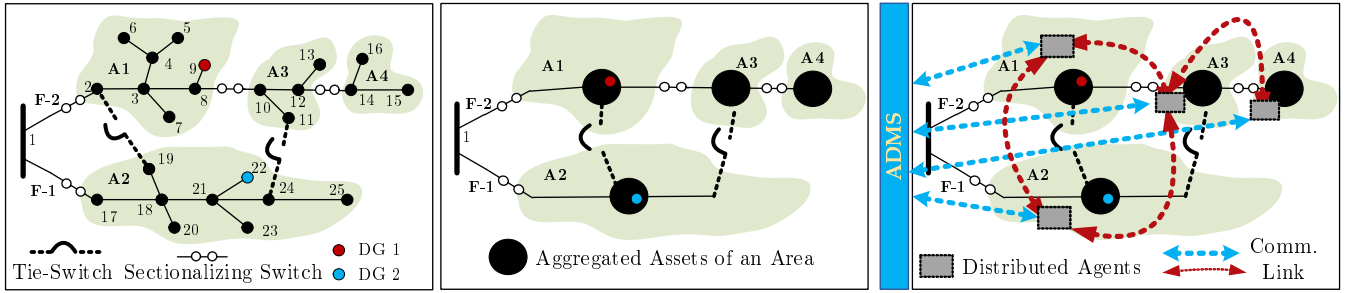
Fig. 2: (a) Example network with 25 nodes. (b) Switch Level Equivalent Model (SLEM) for the example network: all the assests within areas are aggregated. (c) Communication links among Layer-1 and Layer-2 agents
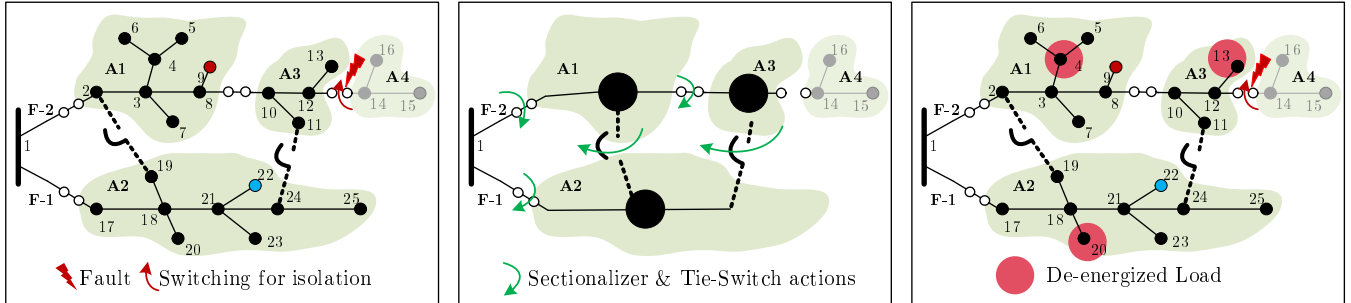

Fig. 3: (a) Fault isolation for example network. (b) Stage-I: Layer-1 agent optimizes sectionalizer & tie-switch actions for reduced-order SLEM network. (c) Stage-II: Layer-2 agents optimizes load switch statuses for respective areas

MILPs are solved in a distributed manner using local federated information for optimal restoration.

2) Distributed Optimization Algorithm: The traditional distributed optimization algorithms require a large number of macro-iterations (~ 100) among distributed agents [5]. On the contrary, the distributed algorithms that use problem structure for decomposition and information sharing reduce the number of communication rounds among distributed agents (macro-iterations) drastically [19], [21]. Thus, here we use a specialized problem decomposition using the power flow structure in a radially operated power distribution system. Specifically, we used the information from the upstream area (UA) and downstream area (DA) for the radially operated grid to design an information-sharing protocol that leads to faster boundary variables. In this case, DA and UA are seen as equivalent load and voltage source, respectively. Each distributed agent solves the local MILP for the switch-delimited area and then exchanges the computed shared bus quantities with its immediate neighbors. The process is repeated until the power flow variables convergence at the UA-DA boundary.

It is to be noted that the proposed distributed coordination approach differs from a similar approach used in [19]. First, unlike proposed algorithm in [19], which requires specifying unique UA-DA pairs, the proposed distributed approach in this paper is used for restoration with changing network operational topologies based on the statuses of sectionalizing and tie switches. Thus, a careful decomposition of the central optimization problem is required. To this end, the proposed distributed coordination approach uses the Stage-I algorithm to establish the parent-child relation among the switch-delimited areas. Second, restoration is a MILP problem with integer decision variables that require specialized information sharing among UA-DA pairs, unlike continuous-only decision-make

problem in [19]. Thus, we identify additional information that needs to be exchanged among UA-DA pairs to motivate fast convergence of the boundary variables.

III. STAGE-I: FORMING RESTORED NETWORK

This section details Stage-I of the proposed method where the Layer-1 agent optimizes for a restored network topology for the distribution system.

A. Network Model

Let, the power distribution network be modeled as an undirected graph $\mathcal{G} = (\mathcal{V}, \mathcal{E})$; the set $\mathcal{V}$, with cardinality $|\mathcal{V}| = n$ representing buses, and the set $\mathcal{E}$, with cardinality $|\mathcal{E}| = m$ representing edges associated with the physical electrical lines. However, the Layer-1 agent requires the SLEM model of the network, and thus, Stage-I of the algorithm is solved using a reduced-order network model (Fig. 2b). All buses within the sectionalizer switch-delimited area are aggregated (represented as a single equivalent node) and communicated to Layer-1 agent from corresponding Layer-2 agent. After the fault clearance, Stage-I of the algorithm is initialized where, Layer-1 agent solves the MILP for a reduced-order graph $\mathcal{G}_t = (\mathcal{V}_t, \mathcal{E}_t)$, where the cardinality $|\mathcal{V}_t|$ is equal to the number of healthy sections of the network (see Fig. 3a-3b).

B. Stage-I Problem Formulation

In Stage-I, the problem objective is to form a restored tree/forest to supply all the loads in the grid after fault isolation. Specifically, a graph-theoretic method is introduced to obtain the optimal restored network topology. The integer variables associated with the topological constraints are decided at this stage to obtain the radially-operated optimal

---

Stage-I Optimization Problem: Restored Network Topology

Maximize: Maximize $\sum\limits_{j \in \mathcal{V}_t} \sum\limits_{\phi \in \{a,b,c\}} u_j \; \mathcal{P}_{Lj}^{\phi}$ (1)

Subject to:
- Tree topology
$$\sum_{e \in \mathcal{E}_c} \delta_e \le |\mathcal{E}_c| - 1, \qquad \forall e \in \mathcal{E}_c \tag{2}$$
- Connectivity Constraints
$$u_i = 1, \forall i \in \mathcal{V}_t \tag{3a}$$
$$\delta_e \le u_i, \quad \delta_e \le u_j, \forall e \in \mathcal{E}_t \tag{3b}$$
$$\delta_e = 0, \quad \forall e \in \mathcal{E}_{Fo} \tag{3c}$$
$$\delta_e = 1, \quad \forall e \in \mathcal{E}_{Fc} \tag{3d}$$
- Flow conservation
$$\sum_{e:(i,j) \in \mathcal{E}_t} \delta_e \, \boldsymbol{P}_e = \boldsymbol{P}_{Lj} + \sum_{e:(j,k) \in \mathcal{E}_t} \delta_e \, \boldsymbol{P}_e \tag{4a}$$
$$\sum_{e:(i,j) \in \mathcal{E}_t} \delta_e \, \boldsymbol{Q}_e = \boldsymbol{Q}_{Lj} + \sum_{e:(j,k) \in \mathcal{E}_t} \delta_e \, \boldsymbol{Q}_e \tag{4b}$$
$$\boldsymbol{P}_e \le \boldsymbol{P}_e^{max}, \quad \forall e \in \mathcal{E}_{fed} \tag{4c}$$
$$\sum_{\forall e \in \mathcal{E}_{fed}} \boldsymbol{P}_e^{max} = \sum_{i \in \mathcal{V}_t} \sum_{\phi \in \{a,b,c\}} u_i \, \mathcal{P}_{Li}^{\phi} \tag{4d}$$

$\mathcal{P}_{Lj}, \; Q_{Lj}$: Aggregated 3-phase load between two switches.

---

restored network topology. The UA-DA relation between areas is also established for the corresponding reconfigured network.

The objective is to maximize the amount of aggregated load restored as defined in (1). Note that a binary variable (u_j) is associated with each healthy section of the reduced-order graph. If multiple sources exist in the system (Feeders and/or DERs), none of the SLEM nodes are energized using more than one source to ensure a radial topology. Thus, any loop formation in the network is avoided using constraint (2). All the healthy sections of the feeder are energized in Stage-I as ensured by (3a). Equation (3b) ensures that if a switch is closed, the buses connecting a switch must be energized and belong to the same source. Next, the faults and the open switches in the distribution network are modeled using (3c). Note that any unknown status of a tie-switch can also be modeled using (3c); a tie-switch with unknown status will be treated as open and will not be included as a decision variable in the reconfiguration problem. On the other hand, some switches might be faulty which are in the closed state and are not controllable. The position of these switching devices is fixed (treated as in the closed state) while solving the optimization (See (3d)). Furthermore, if any switch fails to operate while implementing the restoration solution, then the optimization problem needs to be re-run with the remaining switches as a decision variable. The operational constraints such as the nodal voltage limit of the network are disregarded at this stage; but, the power balance constraints are included as shown in (4a)-(4b). Any node with at least one path that connects it to one of the sources (Feeder/DG) becomes a part of the reduced-order SLEM network (See Fig. 3b). The feeder power supply $\boldsymbol{P}_e, \; \forall e \in \mathcal{E}_{fed}$ is constrained using (4c). However, the feeder power supply limit, $\boldsymbol{P}_e^{max}$, is relaxed at

Stage-I to match it with the total load requirements. Thus, $\sum \boldsymbol{P}_e^{max}$ represents the total loads in the healthy sections of the feeder (See (4d)).

In addition, if DG islanding is necessary due to multiple faults within the feeder, the problem is solved in a similar way where all the DGs are connected to the substation node, representing them as virtual feeders. Thus, each grid-forming DG represents a virtual feeder in $\mathcal{G}_t$. The flow capacity constraints on the virtual feeders are based on the ratio of power capacity of respective DGs and the available feeder capacity, i.e., $\boldsymbol{P}_e^{max}$ is set proportional to the respective size of the DGs. Thus, the DG power capacities dictate the size of the intentional islands that can be supported in the restoration process. Specifically, let $\mathcal{G}_t$ has a total load of P_{tot} and there are n_d numbers of grid forming DGs in the network. Let $\sum P_{feeder}$ be the actual total real power supply available from healthy feeders. Then, the imposed power capacity on a DG is given by (5).

$$\boldsymbol{P}_e^{max} = \frac{P_{Dg,i}}{P_{Dg,1} + .. + P_{Dg,n_d} + \sum P_{feeder}} \times P_{tot} \tag{5}$$

Similarly, the feeder capacity for any healthy feeder will also be relaxed as,

$$\boldsymbol{P}_e^{max} = \frac{P_{feeder,i}}{P_{Dg,1} + .. + P_{Dg,n_d} + \sum P_{feeder}} \times P_{tot}. \tag{6}$$

As shown in (1)- (4), the optimization problem is a MILP that ensures all the nodes in the healthy section of a distribution system are energized using one or multiple sources.

IV. STAGE-II: OPTIMIZE FOR NETWORK OPERATIONS

Stage-I provides the radial restored network or the reconfigured radial distribution system capable of supplying all the loads in the healthy sections of the grid after isolating the faulted zone. Once a restored network is determined, optimal operations of load switches in each area are solved separately by respective distributed agents. The distributed agents for each area interact with their immediate neighbors and run consensus updates to reach the final optimal solution. The consensus is contingent upon the satisfaction of the network's power flow and operating constraints to an operationally feasible restored network. These agents solve a distributed optimization problem using peer-to-peer communication with their immediate neighbors. Each area solves the local optimization problem and then exchanges a minimum set of information among its neighbors and achieves a consensus on the boundary variables over multiple macro-iterations.

The detailed algorithm for the Stage-II is discussed using: (i) the network model & problem formulation for the second stage, (ii) the approximations taken by distributed agents, and (iii) algorithm executed by Layer-2 distributed controllers.

A. Network Model & Problem formulation

A distributed agent has the visibility of their regional/partial network. We denote $\mathcal{E}_{area}$ and $\mathcal{V}_{area}$ as the set of lines and buses in the regional/partial network available to distributed agents. The shared bus with UA is assumed as the slack bus, and the DAs are replaced with lumped loads. The local

This article has been accepted for publication in a future issue of this journal, but has not been fully edited. Content may change prior to final publication. Citation information: DOI 10.1109/TII.2022.3177464, IEEE Transactions on Industrial Informatics

6   IEEE TRANSACTIONS ON INDUSTRIAL INFORMATICS, VOL. XX, NO. XX, XXXX

Stage-II Optimization Problem: Local OPF Sub-Problem (D1)

Maximize:
$$\sum_{i \in \mathcal{V}_S} \sum_{\phi \in \{a,b,c\}} s_i \, w_i P_{Li}^{\phi} \tag{7}$$

Subject to:
$$s_i \leq v_i, \quad \forall i \in \mathcal{V}_S \tag{8a}$$
$$s_i = v_i, \quad \forall i \in \mathcal{V}_{area} \backslash \mathcal{V}_S \tag{8b}$$
$$\sum_{e:(i,j)\in\mathcal{E}} \boldsymbol{P}_e = s_j \, \boldsymbol{P}_{Lj} + \sum_{e:(j,i)\in\mathcal{E}} \boldsymbol{P}_e \tag{9a}$$
$$\sum_{e:(i,j)\in\mathcal{E}} \boldsymbol{Q}_e = s_j \, \boldsymbol{Q}_{Lj} + \sum_{e:(j,i)\in\mathcal{E}} \boldsymbol{Q}_e \tag{9b}$$
$$\boldsymbol{U}_i - \boldsymbol{U}_j = 2(\tilde{\mathbf{r}}_e \boldsymbol{P}_e + \tilde{\mathbf{x}}_e \boldsymbol{Q}_e), \quad \forall e \in \mathcal{E}_{area}\backslash(\mathcal{E}_S \cup \mathcal{E}_R) \tag{10a}$$
$$V_j^{\phi} = a_{\phi} V_i^{\phi}, \tag{10b}$$
$$\boldsymbol{U}_j = A^{\phi} \boldsymbol{U}_i, \quad \forall : (i,j) \in \mathcal{E}_R \tag{10c}$$
$$q_{cap,i}^{\phi} = u_{cap,i}^{\phi} q_{cap,i}^{rated,\phi} U_i^{\phi} \tag{11}$$
$$v_i \boldsymbol{U}^{min} \leq \boldsymbol{U}_i \leq v_i \boldsymbol{U}^{max}, \quad \forall i \in \mathcal{V}_{area} \tag{12}$$
$$(\boldsymbol{P}_e)^2 + (\boldsymbol{Q}_e)^2 \leq \left(\boldsymbol{S}_e^{rated}\right)^2, \quad \forall e \in \mathcal{E}_{area}\backslash\mathcal{E}_S \tag{13}$$
$$-\sqrt{3}\,(\boldsymbol{P}_e + \boldsymbol{S}_e) \leq \boldsymbol{Q}_e \leq -\sqrt{3}\,(\boldsymbol{P}_e - \boldsymbol{S}_e), \quad \forall e \in \mathcal{E}_{area}\backslash\mathcal{E}_S \tag{14a}$$
$$-\sqrt{3}/2\,\boldsymbol{S}_e \leq \boldsymbol{Q}_e \leq \sqrt{3}/2\,\boldsymbol{S}_e, \quad \forall e \in \mathcal{E}_{area}\backslash\mathcal{E}_S \tag{14b}$$
$$\sqrt{3}\,(\boldsymbol{P}_e - \boldsymbol{S}_e) \leq \boldsymbol{Q}_e \leq \sqrt{3}\,(\boldsymbol{P}_e + \boldsymbol{S}_e), \quad \forall e \in \mathcal{E}_{area}\backslash\mathcal{E}_S \tag{14c}$$
$$\boldsymbol{P}_e \leq \boldsymbol{P}_e^{max}, \quad \forall e \in \mathcal{E}_{fed} \tag{15}$$

$\tilde{\mathbf{r}}_e = \text{Real}\{\alpha\alpha^H\} \otimes \mathbf{r}_e + \text{Im}\{\alpha\alpha^H\} \otimes \mathbf{x}_e, \tilde{\mathbf{x}}_e = \text{Real}\{\alpha\alpha^H\} \otimes \mathbf{x}_e + \text{Im}\{\alpha\alpha^H\} \otimes \mathbf{r}_e, \alpha = [1 \quad e^{-j2\pi/3} \quad e^{j2\pi/3}]^T$, $\boldsymbol{S}_e = \boldsymbol{S}_e^{rated}\sqrt{\frac{2\pi/6}{\sin(2\pi/6)}}$; $a_{\phi} = \sum_{i=1}^{32} b_i \, u_{tap,i}^{\phi}$ – turn ratio of a voltage regulator; $u_{tap,i}^{\phi}$ – a binary variable defined for each step position, i.e., $\sum_{i=1}^{32} u_{tap,i}^{\phi} = 1$; b_i is an incremental voltage value for each tap $b_i \in \{0.9, 0.90625, ..., 1.1\}$; and A^{ϕ} is the square of (a^{ϕ}).

optimization problem solved by the distributed agents at the second stage is defined in Problem (D1). Here, constraint (8) represents the model for the switch variables. If the bus i is $\in \mathcal{V}_S$, then the load at bus i can be energized, de-energized, or partially energized. Equation (9) represents the approximated power flow equations, which is a linearized branch-flow model for the unbalanced distribution system. Constraint (10) models the voltage regulators in the network. The constraints for capacitors and operational limits are described by (11)-(15). The load pick-op variables/switches are set as binary variables, i.e., $s_i \in \{0, 1\}$ for all loads in the network. However, those approximated lumped loads – that are used to estimate DAs have a continuous switch variable, bounded from 0 to 1, i.e., $s_i = [0, 1]$. We assume that the associated switches are capable of operating at any value between 0 and 1 to assess what percentage of load can be supplied by an area to its DAs after optimizing the local area. The distributed optimization algorithm for Stage-II is described next.

B. Distributed Optimization for Service Restoration

The radial tree given by Stage-I dictates the data sharing among agents. Each area has a unique upstream parent region

Algorithm 1:

Stage-II – Distributed Optimization for Restoration

Area	: For Area B
Iteration Count	: k
Receive	: $\{\boldsymbol{U}_n^{(k-1)}, P_n^{(k-1)}\} \in \mathbb{R}^6$ from UA & $\{P_{2,c}^{(k-1)}, Q_{2,c}^{(k-1)}\} \in \mathbb{R}^6$ from C DA
Transmit	: $\{P_{2,B}^{(k)}, Q_{2,B}^{(k)}\} \in \mathbb{R}^6$ to UA and $\{\boldsymbol{U}_{m_j}^{(k)}, P_{m_j}^{(k)}\} \in \mathbb{R}^6$ to j^{th} DA (Area C)
Steps	:

1 **If:** $k = 1$, Area B assumes boundary variables to nominal values

2 **Else:** At iteration count k, Area B receives boundary variables from UA and DAs

3 Area B assumes a fixed voltage $\boldsymbol{U}_s = \boldsymbol{U}_n^{(k-1)}$ at approximated slack node

4 Area B assumes aggregated load $\mathbf{P}_{Lm_j} = \mathbf{P}_{2,c}^{(k-1)}$ and $\mathbf{Q}_{Lm_j} = \mathbf{Q}_{2,c}^{(k-1)}$ at node m_j

5 Area B assumes a limited power supply of $\mathbf{P}_e^{max} = \mathbf{P}_n^{(k-1)}$ from its approximated slack node

6 Solves the OPF problem **(D1)**

7 Exchange the computed shared boundary variables (Fig. 4)

8 Check residual of boundary variable with parent and each j child areas: $\mathcal{R}_j = |\boldsymbol{U}_{m_j}^{(k-1)} - \boldsymbol{U}_{m_j}^{(k)}|$, $\mathcal{R}_p = |\boldsymbol{U}_n^{(k-1)} - \boldsymbol{U}_n^{(k)}|$

9 Calculate error: $\epsilon = \max(\mathcal{R}_j, \mathcal{R}_p)$

10 **If:** $\epsilon \leq$ *tolerance*, then stop iteration for Area B and dispatch decision variables

11 **Else:** Increase iteration count $k \leftarrow k + 1$ & go to step (1)
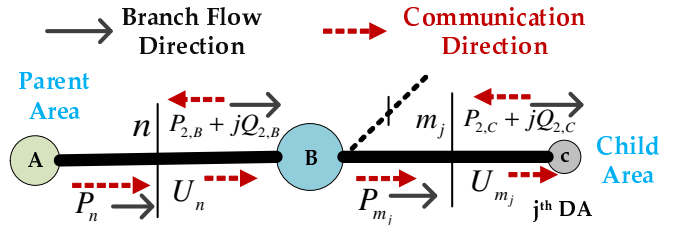

Fig. 4: Stage-II: Communication among distributed agents.

(UA) and/or downstream children areas (DAs). Layer-2 agents at UA computes the shared node voltages after solving the local OPF and sends that variable to respective DA's Layer-2 agent. These Layer-2 agents at DA, models the shared node with UA as a fixed voltage source for its computation. Thus, while solving (D1) in its switch-delimited area, agents approximate the upstream network with a fixed voltage source. Likewise, DA's Layer-2 agent computes and shares the required power for their switch-delimited areas with their unique UA by solving corresponding (D1) problem. Using that power, the DAs are approximated as fixed aggregated loads for the regional OPF. Besides the computed shared node voltage, UA also shares the amount of load it can supply without violating the network constraints. After several rounds of information exchange among Layer-2 agents of neighboring areas, the distributed agents reach a consensus on the boundary bus variables and then dispatches the decision variables in respective areas – that are executed by Layer-3 agents.

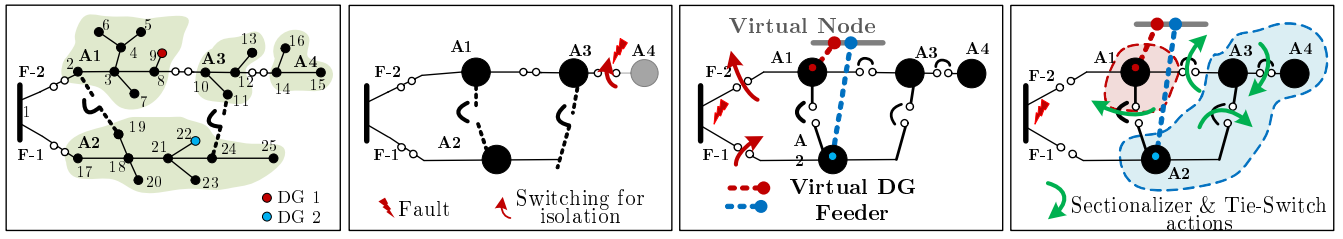This is further elaborated using an example. Lets assume

This article has been accepted for publication in a future issue of this journal, but has not been fully edited. Content may change prior to final publication. Citation information: DOI 10.1109/TII.2022.3177464, IEEE

Transactions on Industrial Informatics

RABAYET *et al.*: LAYERED COORDINATION ARCHITECTURE FOR RESILIENT RESTORATION OF POWER DISTRIBUTION SYSTEMS 7

Fig. 5: (a) TS-1, (b) Fault Scenario 1 (FS-1), (c) Fault Scenario 2 & 3 (FS-2, 3), (d) Optimal sectionalizer & tie-switch actions to form DG islands
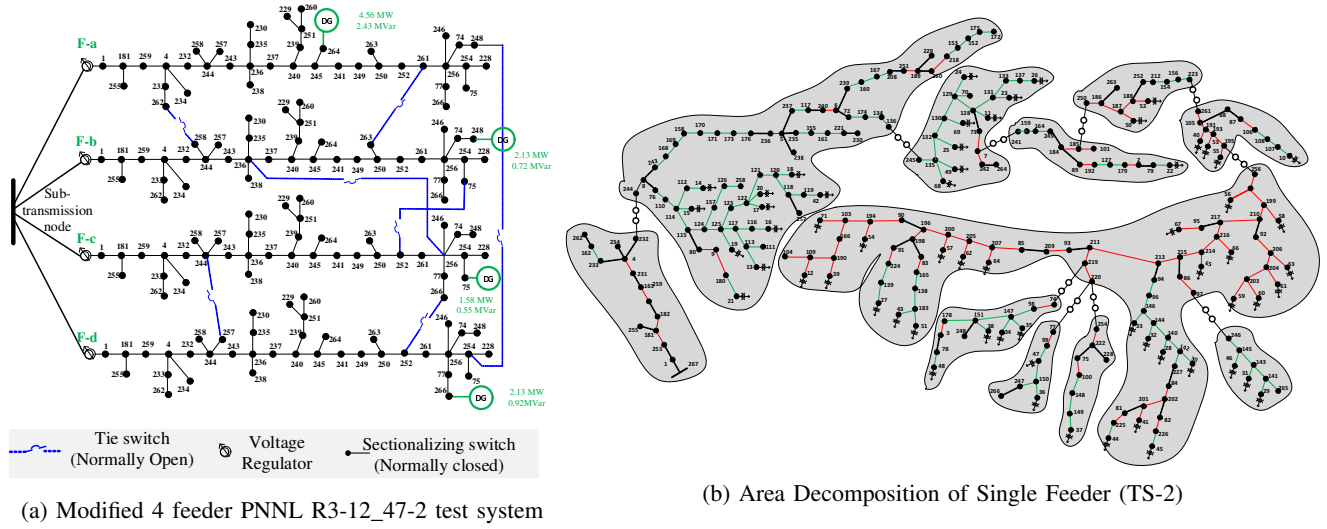

(a) Modified 4 feeder PNNL R3-12_47-2 test system

(b) Area Decomposition of Single Feeder (TS-2)

Fig. 6: TS-2 with area decomposition shown in a single feeder

TABLE I: Fault Scenarios

System	Scenario	Faulted Line	Islanding	Power Limit (MW)
TS-1	FS-1	Line 12-14	No	0.276
	FS-2	Substation	Yes	0.324
	FS-3	Substation	Yes	0.288
TS-2	FS-4	Line 245-241	No	16.20
	FS-5	Line 245-241	No	14.40
	FS-6	Multiple	Yes	9.45
	FS-7	Multiple	Yes	8.40

a small segment of the network containing Area A, B, and C (Fig. 4). Let C be the jth DA of Area B. Also, Area B shares the boundary node n with A, and node m_j with its jth child Area C. We denote any edge e with received end bus number, i.e., $\mathbf{P}_n + j\mathbf{Q}_n$ and $\mathbf{P}_{m_j} + j\mathbf{Q}_{m_j}$ as the three-phase complex power flow, that can be delivered by Area A and B to bus n and m_j, respectively, upon solving OPF for respective areas. $\mathbf{P}_n + j\mathbf{Q}_n$ and $\mathbf{P}_{m_j} + j\mathbf{Q}_{m_j}$ are used as a power supply constraint for Area B and C, respectively. Similarly, subscript $\{2, C\}$ for $\mathbf{P}, \mathbf{Q}$ indicates the branch flow from the approximated slack node, computed by Area C. This is the required power for given constraints in the respective area. The squared magnitude of three-phase voltages at node n and m_j are represented $\boldsymbol{U} = |\boldsymbol{V}|^2$ with respective subscripts. In Stage-II, Layer-2 agent of Area A computes the optimal voltage of shared node n, $\boldsymbol{U}_n$; and Area B assumes a fixed voltage source at node n with that voltage value of $\boldsymbol{U}_n$, to approximates the whole upstream network. Again, Area B approximates the whole downstream network with aggregated loads of $\mathbf{P}_{2,C} + \mathbf{Q}_{2,C}$, for all child Area C. The active power flow restriction for Area B, computed by the Layer-2 agent of Area A is P_n. Then, the Layer-2 agent of Area B solves local (D1) OPF, and shares corresponding variables with neighbors. Please note that area B has multiple children areas, but for simplicity, we are discussing for any j^{th} child area here. **Algorithm 1** describes the Stage-II for any Area B of the network.

V. SIMULATION RESULTS AND DISCUSSIONS

The proposed LADAR architecture is thoroughly validated using a synthetic 25-node system (TS-1) and a modified four-feeder system using the PNNL R3-12_47-2 test system (TS-2) developed in [22], [23]. All experiments were simulated in Matlab 2018b on a desktop machine with 8GB memory and Core i7-8700 CPU @3.2GHz. The MILP problems in both Centralized Optimal Power Flow (C-OPF) and LADAR models are solved using *IBM CPLEX*. Here, TS-1 is used to explain the proposed algorithm using a small test system. TS-2 with 1069 three-phase buses is used to validate the proposed distributed algorithm's applicability and scalability for larger distribution systems. It is assumed that the test systems are already decomposed at the corresponding sectionalizer switch level and comprised of multiple areas see (Figs. 5a & 6b). TS-1 is comprised of four areas (Fig. 5a) and a single feeder of TS-2 is comprised of 11 areas (see Fig. 6b). Thus the entire TS-2 is comprised of 44 areas. All the fault scenarios have been shown in Table I. The proposed approach is also compared against an equivalent C-OPF model for distribution system restoration problem [4].
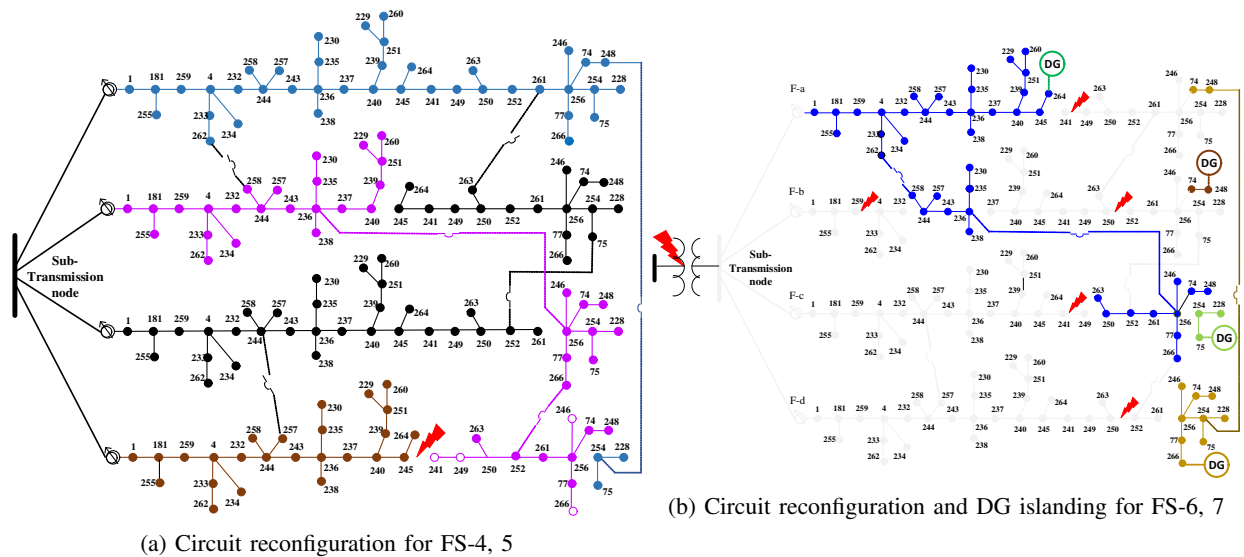
(a) Circuit reconfiguration for FS-4, 5

(b) Circuit reconfiguration and DG islanding for FS-6, 7

Fig. 7: Restoration results with and without DGs. Different Color indicate the feeder reach for laods

A. TS-1: Synthetic 25-node System

In this section, we present the simulated results for the proposed method for different fault-scenarios for TS-1. The synthetic 25-node three-phase test system has total connected three-phase loads of 360 kW.

1) Fault Scenario 1: In the normal operating condition, TS-1 has 2 open tie-switches and 4 closed sectionalizing switches. For FS-1, the fault occurs in a line between node $12 - 14$, and we assumed that the feeders could supply 92 kW of power per phase. The first stage of the method finds the restored network after isolating the faulted area A4 by opening the fault clearing switches. The tie-switch statuses between node $2 - 19$, $12 - 14$ and $11 - 24$ is open while sectionalizing switch between nodes $8 - 10$ is closed. Fig. 5b shows the restored network after Stage-I is complete by ADMS.

At Stage-II, the Layer-2 agents optimize for the load switches within their respective areas by solving the distributed optimization problem detailed in Section V. The number of communication rounds among the neighboring distributed agents is defined as the *macro-iterations*. After consensus at the boundary, the optimal load switch statuses are enacted by respective distributed agents. The results of Stage-II are shown in Table II. From the table, we can see that the solution of distributed agents is comparable to the centralized solutions. Within four macro-iterations, the proposed method reaches convergence to supply 261 kW of total power, which is close to the C-OPF solution of 275 kW.

2) Fault Scenario 2 & 3: Here, we assume a fault at the substation, requiring DGs to intentionally island to supply critical loads. There are 2 grid-forming DGs in the network located at nodes 9 and 22. After the fault isolation, the Layer-1 agent executes the Stage-I algorithm to form the DG islands by opening sectionalizing switch between node $8 - 10$ and closing the tie-switch between node $11 - 24$ (Fig. 5d). The tie-switch between node $2 - 19$ remains open. Note that FS-2 and FS-3 differ in the generation limit of DGs in the network. Both in FS-2 & FS-3, similar to FS-1, after the islands are formed, distributed agents of area A2, A3, and A4 execute

Stage-II of the algorithm. The distributed agents converge to the same boundary variables for the shared buses and dispatch the optimal load switch actions. Since area A1 formed an island itself, the corresponding agent does not communicate with other Layer-2 agents. For the DG islanding cases, the LADAR also attains a solution that is closer to C-OPF. Table II shows that the distributed agents agree on all the boundaries after 3 macro-iterations to supply a total of 281 kW of loads. Here, the maximum DG generation was set to 288 kW. The central solution is able to supply 287 kW. Note that the time required for LADAR is less than the C-OPF compute time. The comparison of active power loads for the LADAR and C-OPF method has been shown in Fig. 8. As can be observed, in FS-2, the limit of active power supply per phase was 108 kW. C-OPF can supply $107.5, 106.1$ & 107.1 kW in phase a,b & c, while LADAR can supply $105.1, 104$ & 105.1 kW of loads. Due to the lack of complete visibility, distributed agents can switch off bigger loads in contrast with C-OPF solutions.

B. TS-2: 4 Feeder PNNL R3-12.47-2 System

This section demonstrates the efficacy and scalability of the proposed scheme using a large three-phase TS-2 system with 1069 buses. We present and compare the simulated result for four different fault scenarios. The simulated results are compared with the solutions of C-OPF to validate the developed DSR scheme. Note that some loads in TS-2 are considered critical loads, and for all the cases, these loads are supported by grid/DGs.

1) Fault Scenario 4 & 5: The normal operating scenario for TS-2 is shown in Fig. 6. For FS-3 and 4, the fault occurs at a line between switch $245 - 241$ of the last feeder as depicted in Fig. 7a. In FS-4, it is assumed that the grid can supply 16.2 MW of power, while for FS-5, 14.4 MW of active power supply has been considered. Stage-I obtains the optimal restored network by reconfiguring the network by closing 4 tie-switches (Fig. 7a). The faulted line is isolated, and the reconfigured network can supply power to the system. The

TABLE II: C-OPF vs. LADAR

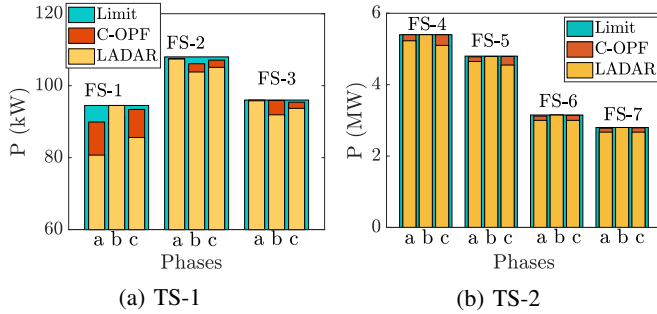| System	Scenario	Macro-Iteration		P_{tot} (MW)		Time (sec)	
		C-OPF	LADAR	C-OPF	LADAR	C-OPF	LADAR
TS-1	FS-1	N/A	4	0.275	0.261	0.242	0.179
	FS-2	N/A	3	0.321	0.316	0.228	0.103
	FS-3	N/A	3	0.287	0.281	0.237	0.145
TS-2	FS-4	N/A	9	16.2	15.8	~ 60	~ 4
	FS-5	N/A	9	14.4	14	~ 60	~ 4
	FS-6	N/A	8	9.4	9.2	~ 2	~ 1
	FS-7	N/A	8	8.4	8.1	~ 2	~ 1

(a) TS-1   (b) TS-2

Fig. 8: Comparison of C-OPF and LADAR in Each Phase

proposed restoration method scales well for large systems. From table II, we see that LADAR only takes 9 macro-iterations and can supply 15.8 MW of power for FS-4, while the C-OPF can supply 16.2 MW. Due to parallel computation, LADAR takes a significantly less time to converge.

2) Fault Scenario 6 & 7: We also demonstrate DG islanding cases for the large-scale distribution system. In FS-6 and FS-7, multiple faults at the substation and other locations are simulated, representing an extreme event. For FS-6 & 7, we assume that the DGs generated a total active power of 9.45 MW and 8.4 MW, respectively. As the network has 4 grid-forming DGs, 4 islands are formed (Fig. 7b). DG located at the first feeder can supply active power to a part of feeders 2 and 3. DGs at feeders 2 and 3 form islands and supply local loads only. DG at feeder 4 supplies load to a small part of the feeder 1. The optimal solution is then compared with the solutions with the C-OPF solutions. While C-OPF can supply 8.4 MW of load for FS-7, LADAR can support 8.1 MW of loads. For all the simulated scenarios, the power supply is restored to the critical loads.

VI. DISCUSSIONS

A. Effect on Reliability Indices

The reliability indices such as System Average Interruption Duration Index (SAIDI), Customer Minutes of Interruptions (CMI), and Customer Average Interruption Duration Index (CAIDI) depend on restoration time after the fault has occurred. To evaluate these indices, the total duration and frequency of outages for a feeder should be evaluated for a given period of time, for example, a year. Furthermore, the evaluation of these indices becomes more challenging when distribution automation with remote-controlled switches and self-healing system is in place [24]. The restoration implementation uses a sequence of switching operations to restore interrupted customers and the restoration time of different customers can be different [25]. In what follows, we describe

how the proposed approach can help utilities to improve their reliability indices.

This paper aims to enable a distributed decision-making framework to support the bottom-up restoration of the distribution grid using all available resources, including distributed generation (DGs), while only requiring regional awareness and limited communications with neighboring connected regions. It is demonstrated that the proposed approach is efficient and scalable as compared to the traditional centralized optimization methods. More specifically, the proposed distributed approach will generate a sequence of control actions that optimally coordinate feeder reconfiguration and DG islanding to restore the maximum distribution loads. Therefore, with the execution of the restoration solution generated by the proposed approach, the utility companies can quickly restore the faulted feeders that can help significantly improve the reliability indices.

B. Layered Coordination Architecture

1) Suitability to Modern Distribution Grid Control Environment : Power distribution systems are envisioned to evolve in complexity and scale over time as the "richness" of systems functionality increases thus making the coordination and control of different resources such as DERs, intelligent devices, and agents challenging. This calls for a new architectural approaches that includes digital processing, analytics and control software at many locations in and along the power grid infrastructure to enhance flexibility in grid automation and implement control actions across tens of millions of end points. Towards this goal, the United States Department of Energy (DOE), through the Grid Modernization Initiative (GMI), has driven extensive research in the area of grid architecture to provide a foundation for meeting the evolving needs of distribution planning and control [26]–[30]. An example of such effort is to address the increasing dynamics and complexity of the grid using decentralized and distributed approaches; laminar coordination framework described in [9] follows a distributed system approach for grid control. We adopted the laminar control architecture in the restoration problem as this framework increases operational flexibility by coordinating centralized and distributed control systems [11]. In future, the proposed distributed restoration algorithm can be hosted in a open-source, standards-based application development platform, GridAPPS-D, developed at the Pacific Northwest National Laboratory [10] and this can serve as a foundation for accelerating the development and field implementations of such distributed approaches.

2) Cost-Benefit Analysis: The centralized paradigm is computationally expensive and usually have lower cost for basic system functions. However, it can be expensive to expand and include advanced functions after initial deployment due to lack of interoperability; when a new device/resources is connected to a network, the control algorithms of a central controller need to be updated. In contrast, the distributed controls provide greater interoperability and have the potential to be computationally superior and respect privacy of data and measurements [31]. While the initial cost of distributed controls can be higher, they can be lower to accommodate

future changes while meeting the added need for resilience and scalability [11]. Furthermore, the centralized operational paradigm is highly dependent on potentially long communication links and require communicating with all devices, which can require significant bandwidth [26].

In model-based restoration problem, obtaining high granularity situational awareness (identifying activated protected device or network connectivity and outaged load information) is critical to provide a quick restoration plan [32]. While intelligent devices such as AMI and telemetered sensors are deployed in feeders, the information from these devices can be missing or delayed at the centralized controller due to limitations of communication systems and can compromise system resilience because of delay in the restoration process [33]. In such cases, the proposed layered architecture can coordinate the grid's controllable assets in different layers of agents to support critical services and achieve network-level objectives without the need for an expensive communication and data processing infrastructure.

VII. CONCLUSION

This paper proposes a novel layered architecture for information sharing and distribution system optimization to achieve near-optimal solutions for non-convex OPF problems for safety-critical applications such as restoration. The proposed architecture is extended to include a hybrid restoration algorithm with intentional islanding to support critical loads that leverages federated information from distributed agents to enable autonomy and resilience but maintain system reliability using central control of feeder-level switches. A two-stage approach is proposed, where Stage-I solves a centralized MILP problem to determine optimal restored topology using the switch-level equivalent model, and Stage-II determines granular controls for the respective switch-delimited area using distributed optimization enabled by peer-to-peer communication. The proposed approach is demonstrated using a large-scale three-phase multi-feeder distribution system with and without intentional islanding. The solution quality and compute requirements of the proposed layered architecture are compared with an equivalent centralized optimization problem. It is shown that the proposed framework achieves near-optimal solutions for all test scenarios while reducing the compute requirements at a single agent. Compared to a centralized operational paradigm, the added cost and complexity of layered control architecture are justified by the added resilience to single-point failures, reduced situational awareness requirements, and enabling autonomy using distributed algorithms. Thus, with a move towards a more distributed and decentralized decision-making paradigm in the active power distribution systems, the use of the proposed layered architecture will be crucial to coordinating numerous dispersed and possibly privately-owned decision-making agents.

REFERENCES

[1] Y. Wang, C. Chen, J. Wang, and R. Baldick, "Research on resilience of power systems under natural disasters—a review," *IEEE Transactions on Power Systems*, vol. 31, no. 2, pp. 1604–1613, 2016.

[2] National Academies of Sciences, Engineering, and Medicine and others, *Enhancing the resilience of the nation's electricity system*. National Academies Press, 2017.

[3] A. Golshani, W. Sun, Q. Zhou, Q. P. Zheng, and J. Tong, "Two-stage adaptive restoration decision support system for a self-healing power grid," *IEEE Transactions on Industrial Informatics*, vol. 13, no. 6, pp. 2802–2812, 2017.

[4] S. Poudel and A. Dubey, "Critical load restoration using distributed energy resources for resilient power distribution system," *IEEE Transactions on Power Systems*, vol. 34, no. 1, pp. 52–63, 2018.

[5] D. K. Molzahn, F. Dörfler, H. Sandberg, S. H. Low, S. Chakrabarti, R. Baldick, and J. Lavaei, "A survey of distributed optimization and control algorithms for electric power systems," *IEEE Transactions on Smart Grid*, vol. 8, no. 6, pp. 2941–2962, 2017.

[6] R. Roofegari Nejad and W. Sun, "Distributed load restoration in unbalanced active distribution systems," *IEEE Transactions on Smart Grid*, vol. 10, no. 5, pp. 5759–5769, 2019.

[7] E. Shirazi and S. Jadid, "Autonomous self-healing in smart distribution grids using agent systems," *IEEE Transactions on Industrial Informatics*, vol. 15, no. 12, pp. 6291–6301, 2018.

[8] J. M. Solanki, S. Khushalani, and N. N. Schulz, "A multi-agent solution to distribution systems restoration," *IEEE Transactions on Power systems*, vol. 22, no. 3, pp. 1026–1034, 2007.

[9] J. D. Taft, "Comparative architecture analysis: Using laminar structure to unify multiple grid architectures," Pacific Northwest National Lab.(PNNL), Richland, WA (United States), Tech. Rep., 2016.

[10] R. B. Melton, K. P. Schneider, E. Lightner, T. E. Mcdermott, P. Sharma, Y. Zhang, F. Ding, S. Vadari, R. Podmore, A. Dubey *et al.*, "Leveraging standards to create an open platform for the development of advanced distribution applications," *IEEE Access*, vol. 6, pp. 37 361–37 370, 2018.

[11] K. P. Schneider, S. Laval, J. Hansen, R. B. Melton, L. Ponder, L. Fox, J. Hart, J. Hambrick, M. Buckner, M. Baggu *et al.*, "A distributed power system control architecture for improved distribution system resiliency," *IEEE Access*, vol. 7, pp. 9957–9970, 2019.

[12] F. M. Rodrigues, L. R. Araujo, and D. R. Penido, "A method to improve distribution system reliability using available mobile generators," *IEEE Systems Journal*, 2020.

[13] Y. Shen, C. Gu, Z. Ma, X. Yang, and P. Zhao, "A two-stage resilience enhancement for distribution systems under hurricane attacks," *IEEE Systems Journal*, 2020.

[14] S. Khushalani, J. M. Solanki, and N. N. Schulz, "Optimized restoration of unbalanced distribution systems," *IEEE Transactions on Power Systems*, vol. 22, no. 2, pp. 624–630, 2007.

[15] H. Gao, Y. Chen, Y. Xu, and C.-C. Liu, "Resilience-oriented critical load restoration using microgrids in distribution systems," *IEEE Transactions on Smart Grid*, vol. 7, no. 6, pp. 2837–2848, 2016.

[16] A. Sharma, D. Srinivasan, and D. S. Kumar, "A comparative analysis of centralized and decentralized multi-agent architecture for service restoration," in *2016 IEEE Congress on Evolutionary Computation (CEC)*. IEEE, 2016, pp. 311–318.

[17] H. Li, H. Sun, J. Wen, S. Cheng, and H. He, "A fully decentralized multi-agent system for intelligent restoration of power distribution network incorporating distributed generations [application notes]," *IEEE Computational Intelligence Magazine*, vol. 7, no. 4, pp. 66–76, 2012.

[18] F. Shen, Q. Wu, J. Zhao, W. Wei, N. D. Hatziargyriou, and F. Liu, "Distributed risk-limiting load restoration in unbalanced distribution systems with networked microgrids," *IEEE Transactions on Smart Grid*, 2020.

[19] R. Sadnan and A. Dubey, "Distributed optimization using reduced network equivalents for radial power distribution systems," *IEEE Transactions on Power Systems*, 2021.

[20] "About open field message bus (openfmb)." [Online]. Available: https://openfmb.ucaiug.org/Pages/Overview.aspx

[21] N. Derbinsky, J. Bento, V. Elser, and J. S. Yedidia, "An improved three-weight message-passing algorithm," *ArXiv*, vol. abs/1305.1961, 2013.

[22] K. Schneider, Y. Chen, D. Chassin, R. Pratt, D. Engel, and S. Thompson, "Modern grid initiative-distribution taxonomy," *Final report, Pacific Northwest National Laboratory*, 2008.

[23] S. Poudel, A. Dubey, and K. P. Schneider, "A generalized framework for service restoration in a resilient power distribution system," *IEEE Systems Journal*, 2020.

[24] Y. Xu, C.-C. Liu, and H. Gao, "Reliability analysis of distribution systems considering service restoration," in *2015 IEEE Power Energy Society Innovative Smart Grid Technologies Conference (ISGT)*, 2015, pp. 1–5.

[25] S. Poudel and A. Dubey, "A two-stage service restoration method for electric power distribution systems," *IET smart grid.*, vol. 4, no. 5, 2021-10.

This article has been accepted for publication in a future issue of this journal, but has not been fully edited. Content may change prior to final publication. Citation information: DOI 10.1109/TII.2022.3177464, IEEE Transactions on Industrial Informatics

RABAYET *et al.*: LAYERED COORDINATION ARCHITECTURE FOR RESILIENT RESTORATION OF POWER DISTRIBUTION SYSTEMS 11

[26] J. P. Ogle, R. B. Melton, K. P. Schneider, and R. Jinsiwale, "Enhancing responsiveness and resilience with distributed applications in the grid," in *2021 IEEE Rural Electric Power Conference (REPC)*. IEEE, 2021, pp. 15–20.

[27] J. Taft, P. De Martini, and R. Geiger, "Ultra large-scale power system control and coordination architecture," *Pacific Northwest National Laboratory (PNNL)*, 2014.

[28] J. D. Taft, "Architectural basis for highly distributed transactive power grids: Frameworks, networks, and grid codes," Pacific Northwest National Lab.(PNNL), Richland, WA (United States), Tech. Rep., 2016.

[29] M. Vadari, "The future of distribution operations and planning: The electric utility environment is changing," *IEEE Power and Energy Magazine*, vol. 18, no. 1, pp. 18–25, 2019.

[30] J. D. Taft, "Grid architecture: A core discipline for grid modernization," *IEEE power and energy magazine*, vol. 17, no. 5, pp. 18–28, 2019.

[31] D. K. Molzahn, F. Dörfler, H. Sandberg, S. H. Low, S. Chakrabarti, R. Baldick, and J. Lavaei, "A survey of distributed optimization and control algorithms for electric power systems," *IEEE Transactions on Smart Grid*, vol. 8, no. 6, pp. 2941–2962, 2017.

[32] C. Chen, J. Wang, and D. Ton, "Modernizing distribution system restoration to achieve grid resiliency against extreme weather events: An integrated solution," *Proceedings of the IEEE*, vol. 105, no. 7, pp. 1267–1288, 2017.

[33] Y. Jiang, C.-C. Liu, M. Diedesch, E. Lee, and A. K. Srivastava, "Outage management of distribution systems incorporating information from smart meters," *IEEE Transactions on Power Systems*, vol. 31, no. 5, pp. 4144–4154, 2016.

Kevin P. Schneider (M'06-SM'08-F'20) received his B.S. degree in Physics and his M.S. and Ph.D. degrees in Electrical Engineering from the University of Washington. His main areas of research are distribution system analysis and power system operations. He is currently a Laboratory Fellow at the Pacific Northwest National Laboratory, Manager of the Distribution and Demand Response Sub-Sector, and a Research Professor at Washington State University as part of the PNNL/WSU Advanced Grid Institute (AGI). Dr. Schneider is an Affiliate Associate Professor at the University of Washington and a licensed Professional Engineer in Washington State. He is a Fellow of the IEEE, past chair of the Power & Energy Society (PES) Distribution System Analysis (DSA) Sub-Committee, and the past Chair of the Analytic Methods for Power Systems (AMPS) Committee.

Rabayet Sadnan (S'20) received the B.Sc. and M.Sc. degrees in electrical and electronics engineering from Bangladesh University of Engineering And Technology (BUET), Dhaka, Bangladesh, in 2015 and 2017, respectively. He also received M.Sc. degree in Mathematics from Washington State University (WSU) in 2021. From 2018, he is working as a research assistant with the School of Electrical Engineering and Computer Science, Washington State University (WSU), Pullman, WA, USA. His research interests include renewable energy, microgrid, distribution system analysis, distributed optimization and control.

Shiva Poudel (M'20) received the B.E. degree from the Department of Electrical Engineering, Pulchowk Campus, Kathmandu, Nepal, in 2013, the M.S. degree from the Electrical Engineering and Computer Science Department, South Dakota State University, Brookings, SD, USA, in 2016, and a Ph.D. degree in Electrical Engineering from Washington State University, Pullman, WA in 2020. He is currently a Power Systems Research Engineer at the Pacific Northwest National Laboratory. His research interests include distribution system modeling & analysis, resilience assessment, and the development of new planning and operational tools for power distribution systems.

Anamika Dubey (M'16-SM'21) received her Ph.D. degree in Electrical and Computer Engineering from the University of Texas at Austin in Dec 2015. She is currently an Assistant Professor in the School of Electrical Engineering and Computer Science at Washington State University, Pullman, WA. Her research focuses on the optimization and control of large-scale electric power distribution systems for improved efficiency, flexibility, and resilience. Her expertise is in modeling, analyzing, and operating active power distribution systems with massive penetrations of controllable grid-edge resources (including DERs, EVs, and GEBs). She is a recipient of the National Science Foundation (NSF) CAREER Award. She serves as the Associate Editor for IEEE Transactions on Power Systems, IEEE Power Engineering Letters, and IEEE Access. She is the current secretary of IEEE PES Distribution Systems Analysis Subcommittee and IEEE PES University Education Subcommittee and serves as PES Chapter Chair for the IEEE Palouse Section.